

# Resonance Characteristics and Field Enhancement in Cylindrical Electromagnetic Bandgap Structures

#Vakhtang Jandieri<sup>1</sup>, Kiyotoshi Yasumoto<sup>2</sup> and Yunfei Liu<sup>2</sup>

<sup>1</sup>School of Electrical Engineering and Computer Science  
 Kyungpook National University, Republic of Korea  
 E-mail: jandieri@ee.knu.ac.kr

<sup>2</sup>College of Information Science and Technology  
 Nanjing Forestry University, China  
 E-mail: kyasumoto@kyudai.jp, lyf@njfu.edu.cn

## 1. Introduction

Recently novel electromagnetic bandgap (EBG) structures - cylindrical EBG structures - have received a growing attention because of their potential applications to the designs of beam forming and multibeam antennas [1]. In this paper, excitation of the cylindrical EBG structure by line source located at the origin of the structure and by TM polarized plane waves is studied. Transmission spectra of *eccentric* cylindrical EBG structures are investigated using a rigorous and accurate semi-analytical method based on the cylindrical Floquet mode expansion. The method takes into account all of the cylindrical Floquet modes and their interactions between the layers [2-4]. The resonance and stopbands of the transmission into the several principle Floquet modes are studied. We have numerically shown that when cylindrical EBG structure of *eccentric* configuration is illuminated by a plane wave of particular resonance frequency, enhancement or “shadowing” effects of the field inside the EBG structure are observed and these effects strongly depend on the angle of incidence of the plane waves. Enhancement and “shadowing” effects of the field could be explained from the Reciprocity Relation for the cylindrical structures. To the best of authors’ knowledge, such studies are performed first time.

## 2. Formulation of the Problem

The cylindrical EBG structures are formed by  $N$ -layered *eccentric* cylindrical arrays of circular rods located in a homogeneous background medium with material constants  $\epsilon_0$  and  $\mu_0$  as shown in Fig. 1. The  $M_\nu$  circular rods with radius  $r_\nu$  are periodically distributed on each of  $N$  circular rings with radii  $R_\nu$  ( $\nu = 1, 2, \dots, N$ ). The  $\# \nu$  circular ring with radius  $R_\nu$  separates two cylindrical regions  $(\nu - 1)$  and  $(\nu)$ . The center  $O_1$  of the innermost  $\#1$  ring in the *eccentric* configuration is chosen as the global origin  $O$ . We assume excitation by a line source located at the global origin  $O$  and by the TM polarized plane waves from the outermost  $(N+1)$ -th region.

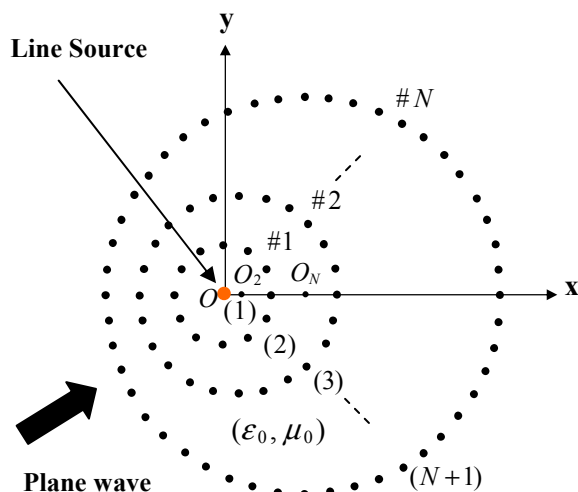


Figure 1: Cylindrical EBG structures of *eccentric* configuration formed by  $M_\nu$  circular rods with radius  $r_\nu$  periodically distributed on each of  $N$  circular rings with radii  $R_\nu$  ( $\nu = 1, 2, \dots, N$ ). Excitation by a line source and TM polarized the plane waves are considered.

The total field in regions ( $\nu$ ) and ( $\nu+1$ ) separated by the  $\nu$ -th layer of the array is expressed in matrix form as follows:

$$E_z^{(\nu)}(\rho, \varphi) = \Phi_\nu^T \cdot \mathbf{b}^{(\nu)} + \Psi_\nu^T \cdot \mathbf{c}^{(\nu)}, \quad E_z^{(\nu+1)}(\rho, \varphi) = \Phi_{\nu+1}^T \cdot \mathbf{b}^{(\nu+1)} + \Psi_{\nu+1}^T \cdot \mathbf{c}^{(\nu+1)} \quad (1)$$

with

$$\Phi_\nu = [J_m(k_0 \rho_\nu) e^{im\varphi}], \quad \Psi_\nu = [H_m^{(1)}(k_0 \rho_\nu) e^{im\varphi}], \quad \mathbf{b}^{(\nu)} = [b_m^{(\nu)}], \quad \mathbf{c}^{(\nu)} = [c_m^{(\nu)}] \quad (2)$$

$$\Phi_{\nu+1} = [J_m(k_0 \rho_{\nu+1}) e^{im\varphi_{\nu+1}}], \quad \Psi_{\nu+1} = [H_m^{(1)}(k_0 \rho_{\nu+1}) e^{im\varphi_{\nu+1}}] \quad (3)$$

where  $(\rho_\nu, \varphi_\nu)$  and  $(\rho_{\nu+1}, \varphi_{\nu+1})$  denote the local polar coordinates systems with their origins at the centers of the  $\# \nu$  and  $\#(\nu+1)$  rings. In Eqs.(1) and (2)  $\{b_m^{(\nu)}\}$  represents the unknown amplitudes of the *incoming* cylindrical waves,  $\{c_m^{(\nu)}\}$  are those of the *outgoing* cylindrical waves,  $J_m$  and  $H_m^{(1)}$  are the Bessel and Hankel functions of the  $m$ -th order. The superscript  $T$  denotes the transpose of the indicated vectors. For the *eccentric* configuration of cylindrical EBG structure, when the basis functions in the cylindrical harmonic expansion are different in two regions, the basis functions in region ( $\nu+1$ ) should be transformed to those in region ( $\nu$ ):

$$\mathbf{U}_{\nu, \nu+1} \cdot \mathbf{c}^{(\nu+1)} = \mathbf{R}_{\nu+1, \nu} \mathbf{U}_{\nu, \nu+1} \cdot \mathbf{b}^{(\nu+1)} + \mathbf{F}_{\nu+1, \nu} \cdot \mathbf{c}^{(\nu)} \quad (4)$$

$$\mathbf{b}^{(\nu)} = \mathbf{F}_{\nu, \nu+1} \mathbf{U}_{\nu, \nu+1} \cdot \mathbf{b}^{(\nu+1)} + \mathbf{R}_{\nu, \nu+1} \cdot \mathbf{c}^{(\nu)}, \quad \mathbf{U}_{\nu, \nu+1} = [J_{m-n}(k_0 d_{\nu, \nu+1})] \quad (5)$$

where  $\mathbf{U}_{\nu, \nu+1}$  is the translation matrix, which transforms  $\Phi_{\nu+1}$  and  $\Psi_{\nu+1}$  to  $\Phi_\nu$  and  $\Psi_\nu$ , respectively and  $d_{\nu, \nu+1}$  denotes the distance between two origins  $O_\nu$  and  $O_{\nu+1}$ . Here  $\mathbf{R}_{\nu+1, \nu}$  and  $\mathbf{F}_{\nu, \nu+1}$  represents the reflection and transmission matrices of the  $\nu$ -th layer of the array for the *incoming* cylindrical waves with  $\{b_m^{(\nu+1)}\}$ , whereas  $\mathbf{R}_{\nu, \nu+1}$  and  $\mathbf{F}_{\nu+1, \nu}$  are the corresponding matrices for the *outgoing* cylindrical waves with  $\{c_m^{(\nu)}\}$ . For a detail calculation procedure for reflection and transmission matrices, the interested readers can refer to the previously published papers [2-4].

In case of line source excitation, the initial field in the innermost region ( $I$ ) is expressed as follows:

$$E_z^i = \frac{i}{4} \Psi^T \cdot \mathbf{c}^{(I)}, \quad \mathbf{c}^{(I)} = [\delta_{m0}] \quad (6)$$

After tracing the scattering process over the layers and follow the calculation procedure given in detail in [2-4], the radiated field into the outermost region ( $N+1$ ) shown in Fig.1 is obtained as:

$$E_z^{(N+1)} = \frac{i}{4} \Psi^T \cdot \bar{\bar{\mathbf{F}}}^{(N+1)} \cdot \mathbf{c}^{(I)} \quad (7)$$

where  $\bar{\bar{\mathbf{F}}}^{(N+1)}$  represents the generalized transmission matrix of the  $N$ -layered *eccentric* cylindrical EBG structure from the innermost ( $I$ ) region to the outermost region ( $N+1$ ).

In case of excitation by TM polarized plane wave, the initial field in ( $N+1$ ) region is given:

$$E_z^i = \Phi^T \cdot \mathbf{b}^{(N+1)}, \quad \mathbf{b}^{(N+1)} = [i^m e^{-im\phi^{inc}}] \quad (8)$$

where  $\phi^{inc}$  is the angle of the incidence with respect to the positive  $x$ -axis. The transmitted field in the innermost region ( $I$ ) is given as:

$$E_z^{(I)} = \Phi^T \cdot \bar{\bar{\mathbf{F}}}^{(I)} \cdot \mathbf{b}^{(N+1)} \quad (9)$$

where  $\bar{\bar{\mathbf{F}}}^{(I)}$  represents the generalized transmission matrix of the  $N$ -layered *eccentric* cylindrical EBG structure from the outermost ( $N+1$ ) region to the innermost ( $I$ ) region. The generalized transmission matrices  $\bar{\bar{\mathbf{F}}}^{(N+1)}$  in (7) and  $\bar{\bar{\mathbf{F}}}^{(I)}$  in (9) are obtained the tracing the scattering process over the layers of *eccentric* cylindrical EBG structure. They are expressed exclusively by the reflection  $\mathbf{R}_{\nu, \nu+1}$ ,  $\mathbf{R}_{\nu+1, \nu}$  and transmission  $\mathbf{F}_{\nu+1, \nu}$ ,  $\mathbf{F}_{\nu, \nu+1}$  matrices for each cylindrical layer, their product and inverse operations. It is very important to mention that from the Reciprocity Relation, the following relations between the generalized transmission matrices  $\bar{\bar{\mathbf{F}}}^{(N+1)}$  and  $\bar{\bar{\mathbf{F}}}^{(I)}$  is derived:  $\bar{\bar{\mathbf{F}}}^{(N+1)} = (\bar{\bar{\mathbf{F}}}^{(I)})^T$ .

### 3. Numerical Analysis and Discussions

Although a substantial number of numerical examples could be generated, we discuss here a three-layered structure consisting of the identical circular rods of perfect conductors, where  $r_1 = r_2 = r_3 = 2\text{mm}$ ,  $R_1 = 40\text{mm}$ ,  $R_2 = 2R_1$ ,  $R_3 = 3R_1$ ,  $M_1 = 12$ ,  $M_2 = 24$  and  $M_3 = 36$ . The reflection and transmission matrices were truncated by  $m = n = \pm 16$  after confirming the convergence of solutions. Figure 2 shows the transmission spectra for the *eccentric* configuration of cylindrical EBG shown in Fig. 1, where  $d_{12} = \overline{OO}_2 = 0.1R_1$ ,  $d_{13} = \overline{OO}_3 = 0.2R_1$ . The results for the lowest five modes, which have significant values of the transmission coefficient, are shown in Fig.2. From Fig.2 we can see that there exist a series of stopbands and passbands for each of the excited Floquet modes. The transmission is very small in the stopbands, whereas a sharp resonant peak appears in the passband regions. In the passband regions, there exist special resonance frequencies:  $6.1125\text{GHz}$  and  $6.3\text{GHz}$ , at which the Floquet modes simultaneously resonate.

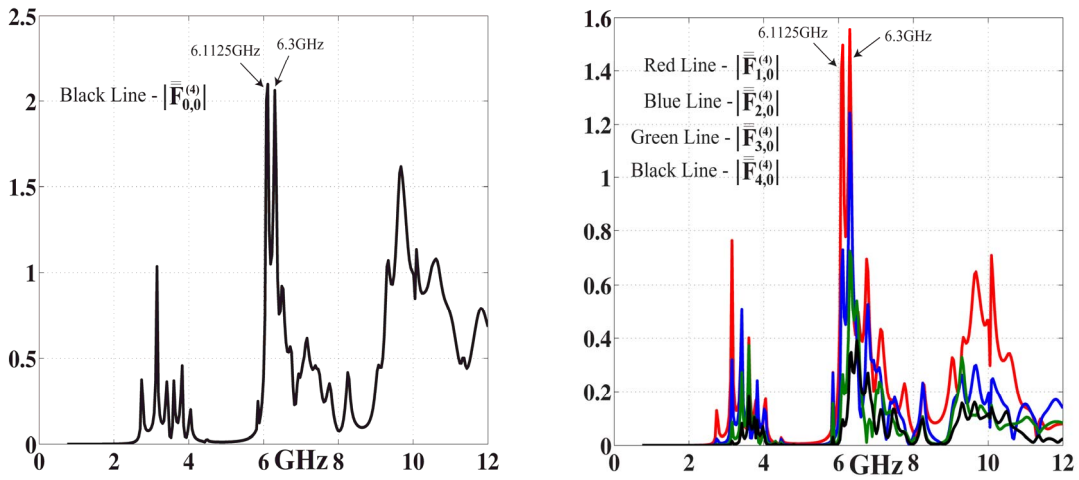
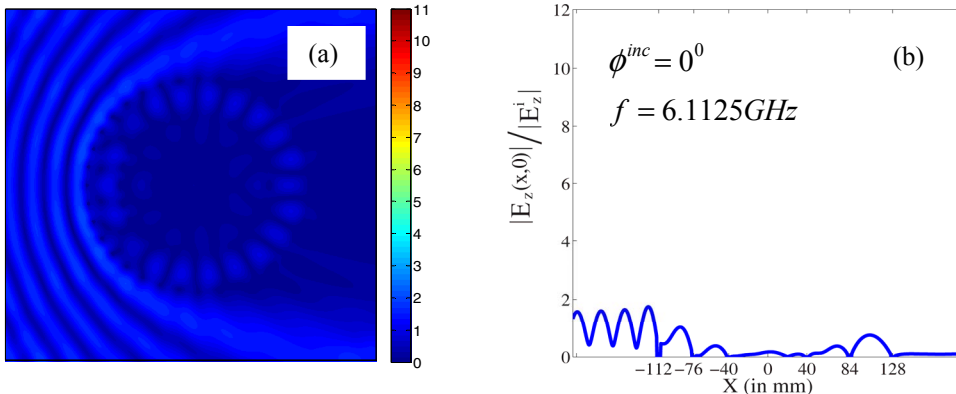


Figure 2: Transmission spectra  $|\overline{F}_{m,0}^{(4)}|$  of Eq.(7) for the *eccentric* three-layered structure cylindrical EBG structure shown in Fig. 1, where  $r_1 = r_2 = r_3 = 2\text{mm}$ ,  $R_1 = 40\text{mm}$ ,  $R_2 = 2R_1$ ,  $R_3 = 3R_1$ ,  $M_1 = 12$ ,  $M_2 = 24$ ,  $M_3 = 36$ ,  $d_{12} = \overline{OO}_2 = 0.1R_1$ ,  $d_{13} = \overline{OO}_3 = 0.2R_1$ .

It should be noted that  $|\overline{F}_{m,0}^{(4)}| = |\overline{F}_{-m,0}^{(4)}|$ . The field distributions inside the cylindrical EBG structure illuminated by a TM plane wave with  $\phi^{inc} = 0^\circ$  and  $\phi^{inc} = 180^\circ$  are plotted for two different excitation frequencies  $f = 6.1125\text{GHz}$  and  $f = 6.3\text{GHz}$  in Figures 3. It could be vividly seen that the “shadowing” effect (a), (e) and the effect of strong enhancement (c), (g) of the field inside the cylindrical EBG structure of *eccentric* configuration are observed and this effect is strongly related to the angle of incidence of plane waves. These features could be very useful to manipulate the electromagnetic properties of a space by surrounding it with a cylindrical EBG structure.



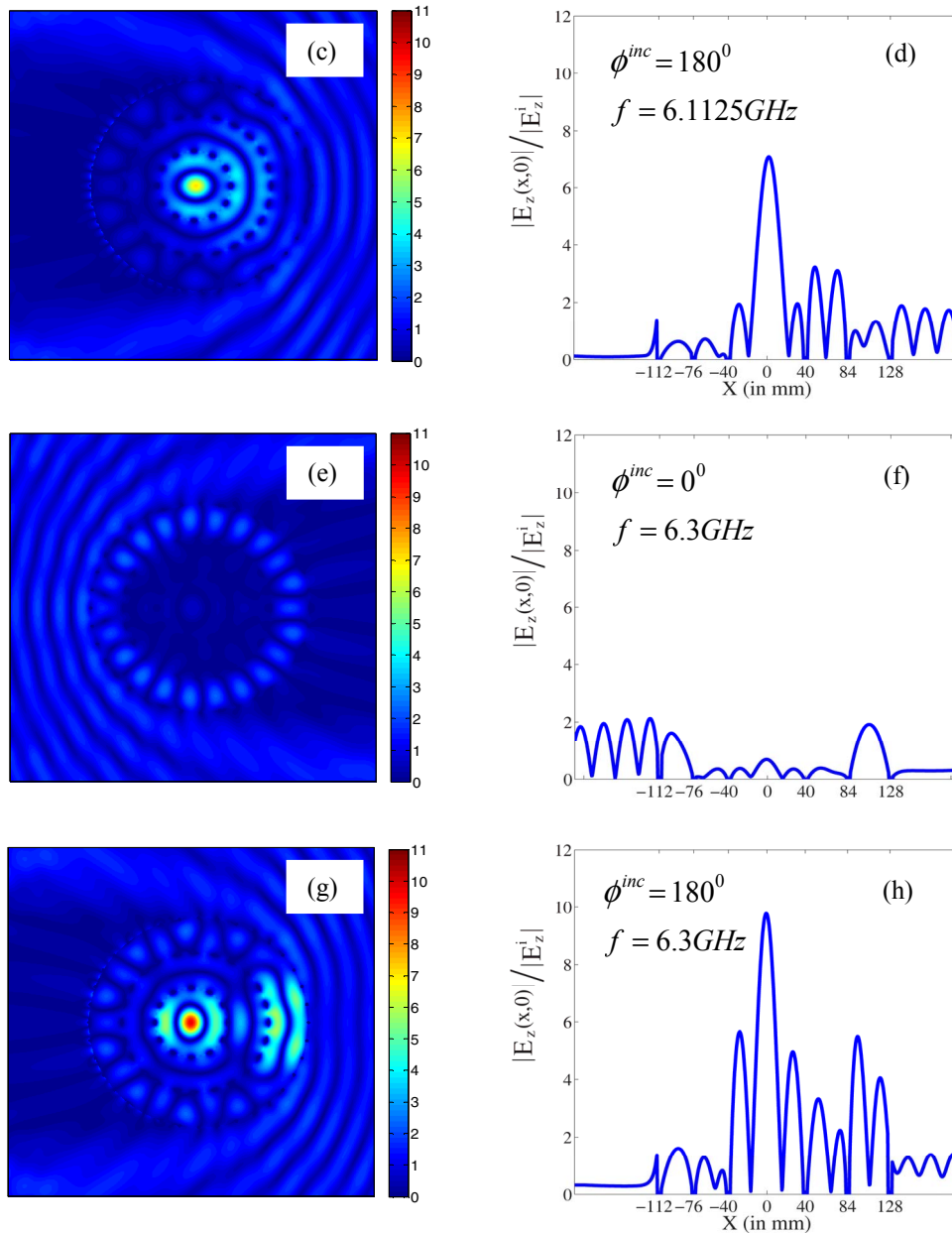


Figure 3: Field distribution in the three-layered cylindrical EBG structure of *eccentric* configuration for the excitation of TM polarized plane wave; (a), (c), (e), (g) - two-dimensional field mapping of  $|E_z(x,y)|$ ; (b), (d), (f), (h) -  $|E_z(x,0)|$  as a function of  $x$ .

## References

- [1] H. Boutayeb and T. Denidni, "Metallic cylindrical EBG structures with defects: Directivity analysis and design optimization," IEEE Trans. Antennas Propag., vol. 55, No. 11, pp.3356-3361, November 2007.
- [2] V. Jandieri and K. Yasumoto, "Electromagnetic Scattering by Layered Cylindrical Arrays of Circular Rods," IEEE Trans. Antennas Propag., vol.59, no.6, pp. 2437-2441, 2011.
- [3] K. Yasumoto, V. Jandieri and B. Gupta, "Guidance and Scattering of Electromagnetic Waves by Layered Cylindrical Arrays of Circular Rods", Proc. IEEE Applied Electromagnetics Conference (AEMC 2009), Kolkata, India, pp.1-4, December, 2009.
- [4] V. Jandieri, K. Yasumoto and Young-Ki Cho, "Rigorous Analysis of Electromagnetic Scattering by Cylindrical EBG Structures," Progress in Electromagnetics Research (PIER), vol.121, pp. 317-342, 2011.